Bioorganic & Medicinal Chemistry 20 (2012) 16–24

Contents lists available at SciVerse ScienceDirect

Bioorganic & Medicinal Chemistry

journal homepage: www.elsevier.com/locate/bmc

Nucleic acid probe containing fluorescent tricyclic base-linked acyclonucleoside for detection of single nucleotide polymorphisms

Kinji Furukawa [a,†], Mayumi Hattori [a,†], Tokimitsu Ohki [a], Yoshiaki Kitamura [a], Yukio Kitade [a], Yoshihito Ueno [b,*]

[a] Department of Biomolecular Science, Faculty of Engineering, Gifu University, 1-1 Yanagido, Gifu 501-1193, Japan
[b] Department of Applied Life Science, Faculty of Applied Biological Sciences, Gifu University, 1-1 Yanagido, Gifu 501-1193, Japan

ARTICLE INFO

Article history:
Received 22 October 2011
Revised 19 November 2011
Accepted 21 November 2011
Available online 1 December 2011

Keywords:
DNA
SNPs
Detection
Acyclonucleoside
Tricyclic base

ABSTRACT

The development of a reliable and simple method for detecting single nucleotide polymorphisms (SNPs), common genetic variations in the human genome, is currently an important research area because SNPs are important for identifying disease-causing genes and for pharmacogenetic studies. Here, we developed a novel method for SNP detection. We designed and synthesized DNA probes containing a fluorescent tricyclic base-linked acyclonucleoside **P**. The type of nucleobases involved in the SNP sites in the DNA and RNA targets could be determined using four DNA probes containing **P**. Thus, this system would provide a novel and simple method for detecting SNPs in DNA and RNA targets.

1. Introduction

The most frequent form of genetic variation in the human genome is a single nucleotide polymorphism (SNP), which occurs roughly once every 1000 bases and is currently thought to be linked to diseases and individual differences in drug response.[1,2] Therefore, the development of a reliable and simple method for detecting SNPs is very important for pharmacogenomics[3] and the realization of personalized medicine. To date, a number of SNP genotyping technologies, such as microarrays,[4,5] molecular inversion probe genotyping,[6] 5′ exonuclease fluorescence-based assay (Taq-Man),[7] pyrosequencing,[8] single-base extension[9] and matrix-assisted laser desorption/ionization time-of-flight mass spectrometry (MALDI-TOF/MS),[10,11] have been developed and applied. Most discrimination principles in these methods are based on differences in the thermodynamic stabilities of the duplexes comprising a probe strand and a complementary DNA target or DNA containing SNPs; the probe binds to the wild-type sequence but not to DNA containing SNPs. However, because differences in duplex stabilities between complementary sequences and sequences containing one base mismatch are small, careful selection of the oligonucleotide probe sequence and the annealing conditions, especially temperature, is needed to prevent genotyping errors.

It would be advantageous to directly detect the formation of base pairing with a target nucleoside, for example, hydrogen bonding with a target nucleobase, as a fluorescence signal in duplex formation. Saito and colleagues reported that oligodeoxynucleotides (ODNs) containing base-discriminating fluorescent (BDF) nucleosides that were modified with a pyrene or dimethylaminonaphthalene residue acted as nucleic acid probes.[12–17] Seitz and colleagues also reported forced intercalation probes (FIT-probes), which contained thiazole orange as a fluorescent base.[18–22]

In this paper, we report a novel method for SNP detection using a nucleic acid probe that contains a fluorescent tricyclic base-linked acyclonucleoside, 8-amino-3-(2,3-dihydroxypropyl) imidazo[4′,5′:5,6]pyrido[2,3-*d*]pyrimidine (**P**) (Fig. 1). The design principle of SNP detection using the nucleoside surrogate **P** is outlined in Figure 2. The fluorescence intensity of the tricyclic base-linked **P** depended on solvent polarity; fluorescence intensity

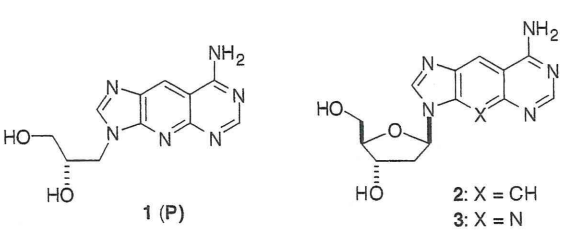

Figure 1. Structures of tricyclic base-linked nucleoside surrogates.

* Corresponding authors. Tel./fax: +81 58 293 2919.
E-mail address: uenoy@gifu-u.ac.jp (Y. Ueno).
† These authors contributed equally to this work.

0968-0896/$ - see front matter © 2011 Elsevier Ltd. All rights reserved.
doi:10.1016/j.bmc.2011.11.045

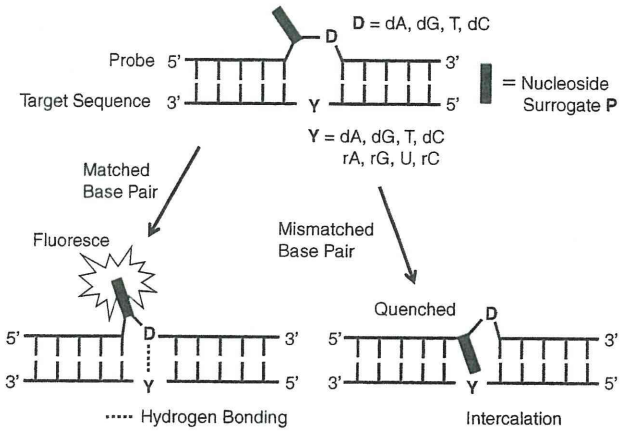

Figure 2. Design principle of SNP detection using the nucleoside surrogate **P**. **Ds** denotes discriminating bases. **Y**s indicates SNP sites.

of **P** was greater in more polar solvents such as methanol and water compared to less polar solvents such as chloroform. Based on this result, we designed nucleic acid probes containing **P** at the 5′ (5′-P-probes) or 3′ sides (3′-P-probes) of discriminating bases **Ds** to produce bulges. It is believed that the inside of the grooves of the DNA helix is more hydrophobic than bulk water.[23] Thus, we presumed that when the **Ds** match the sequences of opposite bases, **Ds** form base pairs with complementary bases, causing the nucleoside surrogate **P** to flip outside the DNA helix and strengthening the fluorescence intensity of **P**. On the other hand, when the mismatched bases have sites opposite of **Ds**, **P** intercalates into the DNA helix because the tricyclic base-linked nucleoside surrogate **P** is more intercalative than natural mono or bicyclic natural nucleobases. This weakens the fluorescence intensity of **P**. We anticipated that we could determine the type of nucleobase involved in the SNP site by comparing the fluorescence intensities of duplexes composed of each probe containing **P**.

2. Results

2.1. Design and synthesis of a fluorescent nucleoside surrogate

Size-expanded nucleoside surrogates **2** and **3** were reported fluoresce under ultraviolet light, emitting fluorescence at ~400 nm.[24–27] Thus, we chose 8-amino-3-(2,3-dihydroxypropyl)imidazo[4′,5′:5,6]pyrido[2,3-*d*]pyrimidine (**P**) as a nucleoside surrogate for this method. We expected that the nucleoside surrogate **P** could be accommodated into a DNA/DNA or DNA/RNA helix without disturbing the local helical structure because **P** is composed of an acyclic three-carbon propylene glycol instead of deoxy-D-ribose, although it carries a size-expanded tricyclic base. We also expected that **P** would flip outside of the helix more easily than natural nucleosides because **P** has a flexible acyclic structure.

The synthesis of the tricyclic base-linked nucleoside surrogate **P** is shown in Scheme 1. 5-Amino-6-cyanoimidazo[4,5-*b*]pyridine (**4**),[28] which was synthesized by a method reported previously, was coupled with (*R*)-2,2-dimethyl-4-(*p*-toluenesulfonyloxymethyl)-1,3-dioxolane (**5**) in the presence of K_2CO_3 in dimethylformamide (DMF) at 60 °C. Only one product was observed on thin-layer chromatography (TLC). After purification on a silica gel column, the product was analyzed by ^1H–^1H correlation spectroscopy (COSY), heteronuclear multiple quantum coherence (HMQC), heteronuclear multiple bond correlation (HMBC) and nuclear overhauser enhancement spectroscopy (NOESY) spectra. In the NOESY experiments, cross-peaks were observed between H2 of the base moiety and the protons of the 1,3-dioxolanylmethyl residue, but no cross-peak was detected between H7 of the base moiety and the 1,3-dioxolanylmethyl portion. From these results, the product was identified as an N3-alkyl derivative **6**. Treatment of **6** with $CH(OEt)_3$ at 100 °C followed by treatment with methanolic ammonia in a steel sealed tube at 110 °C produced an isopropylidene derivative of **P**. The amino group of **7** was protected with a benzoyl group. Deprotection of the isopropylidene group, protection of the primary hydroxy group with 4,4′-dimethoxytrityl (DMTr) group, and phosphitylation produced phosphoramidite unit **12**.

2.2. Photophysical properties of the nucleoside surrogate P

Typical emission spectra of the tricyclic base-linked nucleoside surrogate **P** are shown in Fig. 3. The nucleoside surrogate **P** showed emission maxima at ~390 nm under 332-nm excitation. The fluorescence intensity of **P** depended on solvent polarity; fluorescence intensity of **P** was greater in more polar solvents such as methanol and water compared to less polar solvents such as chloroform. The photophysical data of the tricyclic base-linked nucleoside surrogate **P** are summarized in Table 1. The emission wavelength of **P** was affected by solvent polarity. The emission maximum shifted from 388 nm for chloroform to 399 nm for methanol. The fluorescence quantum yields (Φs) of **P** increased with increasing solvent polarity. The Φ value of **P** was 0.13 in chloroform and 0.97 in water.

2.3. Synthesis of ODNs containing the nucleoside surrogate P

The sequences of ODNs containing the nucleoside surrogate **P** are given in Table 2. CYP2C9 is one of the predominant cytochrome P450 (CYP) enzymes expressed constitutively in the human liver.[29,30] It metabolizes a variety of therapeutically important drugs such as phenytoin, warfarin, and a number of anti-inflammatory drugs, including indomethacin, mefenamic acid, flurbiprofen, ibuprofen, diclofenac, and the oxicams.[29,30] In the present study, we chose the sequence containing an A1075(C) mutation in the *CYP2C9* gene as a model sequence. The probe ODNs were composed of sequences complementary to the *CYP2C9* gene. The probes (5′-P-probes) termed **PA**, **PG**, **PC**, and **PT** contained **P** at the 5′ sides of **Ds**, whereas the probes (3′-P-probes) termed **AP**, **GP**, **CP**, and **TP** possessed **P** at the 3′ sides of **Ds**. Target sequences are abbreviated as S.

All the ODNs containing **P** were synthesized using a DNA/RNA synthesizer. Fully protected ODNs (1.0 μmol each) linked to solid supports were treated with concentrated NH_4OH at 55 °C for 12 h. The ODNs released after treatment were purified by 20% polyacrylamide gel electrophoresis (PAGE) to afford deprotected ODNs. These ODNs were analyzed by MALDI-TOF/MS, and the observed molecular weights were in agreement with their structures.

2.4. Thermal denaturation study and fluorescence experiments of duplexes containing P

First, we examined the ability of the probes to detect SNPs in the DNA targets. The T_m values of the duplexes between the probes and the DNA targets are shown in Table 3 (left column). The highest T_m values were from the duplexes comprising complementary sequences, for example, when the discriminating bases and the target base sequences matched. ΔT_m variation between the matched and mismatched sequences was 3–7 °C. Thus, the discriminating bases possessed sufficient base-selectivity, although they contained the tricyclic nucleoside surrogate **P** at the 5′ or 3′ sides of the discriminating bases.

Fluorescence emission spectra of the duplexes consisting of 5′-P-probes, **PA**, **PG**, **PC**, and **PT** are shown in Fig. 4. Fluorescence

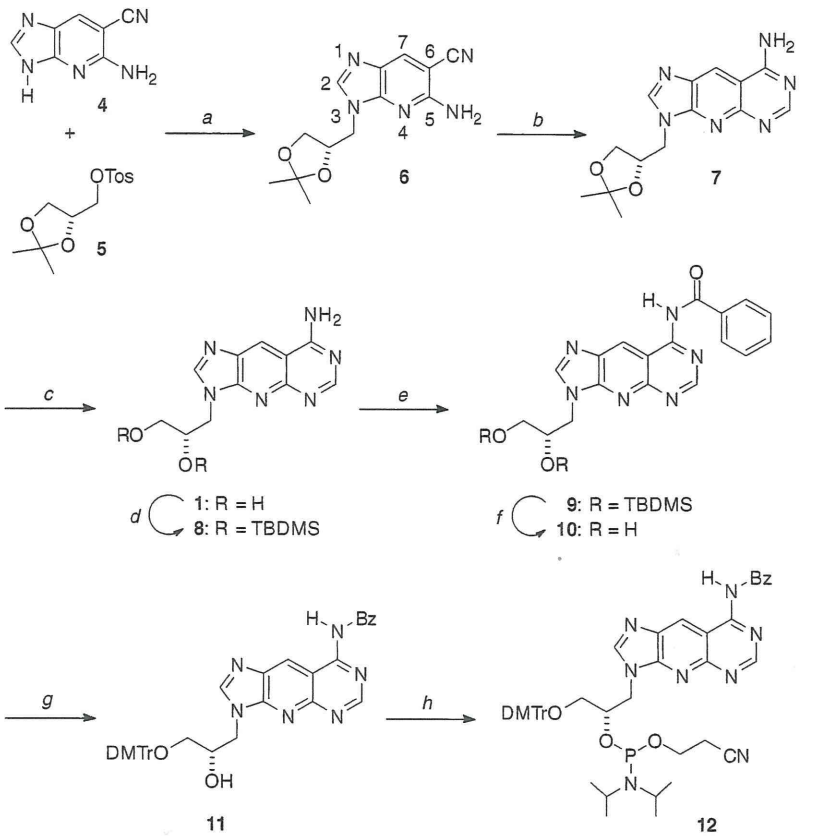

Scheme 1. Reagents and conditions: (a) K_2CO_3, DMF, 60 °C, 70 h, 54%; (b) $HC(OEt)_3$, 100 °C, 54 h; (2) NH_3 in MeOH, 110 °C, 18 h, 65%; (c) CH_3CO_2H, 60 °C, 9 h, 98%; (d) TBDMSCl, imidazole, DMF, rt, 18 h, 81%; (e) BzCl, pyridine, rt, 10 h, 67%; (f) TBAF, THF, rt, 2 h, 75%; (g) DMTrCl, pyridine, rt, 2 h, 56%; (h) chloro(2-cyanoethoxy)(*N*,*N*-diisopropylamino)phosphine, *i*-Pr_2NEt, THF, rt, 30 min, 67%.

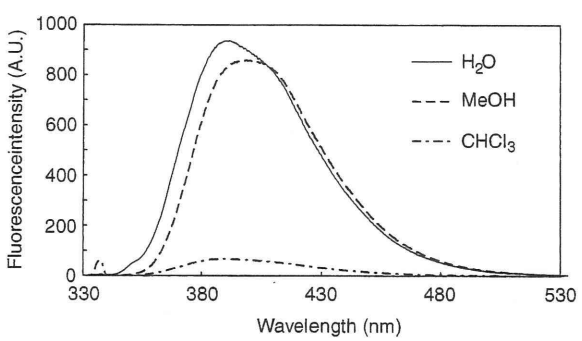

Figure 3. Fluorescence emission spectra of **P** in various solvents. Spectra were obtained under 332-nm excitation on a spectrofluorophotometer in quartz cuvettes with a path length of 1.0 cm at a **P** concentration of 30 μM in an appropriate solvent at 20 °C. Spectra were recorded using an excitation slit of 1.5 nm and emission slit of 1.5 nm.

Table 1
Photophysical properties of **P**. The experimental conditions were described in the Section 4

Solvent	λ_{ex} (nm)	λ_{em} (nm)	ε	Φ
H_2O	333.4	391.6	78.5	0.97
MeOH	335.4	398.6	32.6	0.82
CH_3CN	334.8	386.8	36.2	0.70
EtOAc	336.6	386.4	6.19	0.43
THF	338.8	389.8	7.32	0.19
$CHCl_3$	335.0	388.2	4.70	0.13
CH_2Cl_2	335.0	385.0	8.90	0.12

Φ = fluorescence quantum yield.
ε = dielectric constant.

spectra intensity of the duplexes correlated with the T_m values of the duplexes. In all sequences, the fluorescence intensities were greatest when the discriminating bases were complementary to the target bases. Next, we compared the fluorescence intensities of the duplexes at 390 nm. As shown in Fig. 5 (left column), the fluorescence intensities were greatest when the duplexes were composed of matched sequences: **PA** probe for the SdT target, **PC** probe for the SdG target, **PT** probe for the SdA target, and **PG** probe for the SdC target. However, with the dG target base, fluorescence was also observed for the **PT** probe. This was attributed to a wobble-type base pairing between dG and dT bases.[31] The fluorescence intensities of the single-stranded P-probes were almost equal to those of the mismatched duplexes (data not shown).

The results for probes containing the surrogate **P** at the 3′ side of the discriminating bases (3′-P-probes) are shown in Fig. 6 (left column). Fluorescence intensities of the duplexes were greatest when the discriminating bases were complementary to the target bases (except for the **CP** probe): **AP** probe for the SdT target, **TP** probe for the SdA target, and **GP** probe for the SdC target. No fluorescence was observed with the **CP** probe for the target sequences. From these results, we could determine the type of nucleobases involved in the SNP sites in the DNA targets using the **PA** or **AP** probe for the SdT target, the **PC** probe for the SdG target, the **TP** probe for the SdA target, and the **PG** probe for the SdC target.

Table 2
Oligonucleotide sequences. The underlined letters indicate discriminating bases. The italic letters represent target bases

Abbreviation	Sequence
PA	5′-d(GAA GGT CAA **PA**G TAT CTC T)-3′
PG	5′-d(GAA GGT CAA **PG**G TAT CTC T)-3′
PC	5′-d(GAA GGT CAA **PC**G TAT CTC T)-3′
PT	5′-d(GAA GGT CAA **PT**G TAT CTC T)-3′
PsT	5′-d(GAA GGT CAA **PsT**G TAT CTC T)-3′
AP	5′-d(GAA GGT CAA **AP**G TAT CTC T)-3′
GP	5′-d(GAA GGT CAA **GP**G TAT CTC T)-3′
CP	5′-d(GAA GGT CAA **CP**G TAT CTC T)-3′
TP	5′-d(GAA GGT CAA **TP**G TAT CTC T)-3′
SdA	3′-d(CTT CCA GTT *ACA* TAG AGA)-5′
SdG	3′-d(CTT CCA GTT *GCA* TAG AGA)-5′
SdC	3′-d(CTT CCA GTT *CCA* TAG AGA)-5′
SdT	3′-d(CTT CCA GTT *TCA* TAG AGA)-5′
SrA	3′-r(CUU CCA GUU *ACA* UAG AGA)-5′
SrG	3′-r(CUU CCA GUU *GCA* UAG AGA)-5′
SrC	3′-r(CUU CCA GUU *CCA* UAG AGA)-5′
SrU	3′-r(CUU CCA GUU *UCA* UAG AGA)-5′

Table 3
T_m Values. ΔT_ms [T_m (a duplex between a probe and a complementary target) − T_m (a duplex between a probe and a target containing a mismatched base)] are indicated in parentheses. The experimental conditions are as described in the Section 4

	SdA	SdG	SdC	SdT	SrA	SrG	SrC	SrU
PA	45.6 (−4.5)	47.8 (−2.3)	44.9 (−5.1)	50.1 –	45.0 (−3.1)	47.1 (−1.0)	44.6 (−3.5)	48.1 –
PG	45.8 (−5.8)	45.8 (−5.8)	51.6 –	46.8 (−3.8)	46.8 (−5.5)	47.8 (−4.5)	52.3 –	46.9 (−5.4)
PC	44.5 (−5.6)	52.1 –	44.6 (−5.5)	46.1 (−6.0)	45.5 (−7.7)	51.5 –	44.9 (−6.6)	45.7 (−5.5)
PT	50.5 –	47.1 (−3.4)	45.7 (−4.8)	47.3 (−3.2)	49.2 –	48.0 (−1.2)	44.8 (−4.4)	47.0 (−2.2)
AP	47.8 (−2.5)	46.8 (−3.5)	46.4 (−3.9)	50.3 –	46.5 (−1.4)	49.6 (+1.7)	46.1 (−1.8)	47.9 –
GP	49.1 (−3.5)	47.2 (−5.4)	52.6 –	48.3 (−4.3)	48.1 (−4.7)	48.7 (−4.1)	52.8 –	47.4 (−5.4)
CP	49.8 (−5.1)	54.9 –	48.0 (−6.9)	49.1 (−5.8)	47.2 (−8.9)	56.1 –	48.0 (−8.1)	49.3 (−6.8)
TP	52.4 –	48.9 (−3.5)	47.7 (−4.7)	49.4 (−3.0)	50.0 –	51.7 (+1.7)	48.2 (−2.1)	48.9 (−1.1)

The results for the RNA targets are shown in Table 3 (right column), Fig. 5 (right column), and Fig. 6 (right column). When the discriminating bases and the target bases matched, the T_m values of the duplexes were greatest in all sequences, except for the **AP** and **TP** probes, whose ΔT_m values for duplexes comprising matched and mismatched sequences varied from 1 to 9 °C. Thus, the discriminating bases seemed to have base selectivities in the DNA/RNA duplexes containing the tricyclic nucleoside surrogate **P**. The T_m values of the **AP**/SrG (T_m = 49.6 °C) and **TP**/SrG (T_m = 51.7 °C) duplexes were slightly greater than those of the **AP**/SrU (T_m = 47.9 °C) and **TP**/SrA (T_m = 50.0 °C) duplexes, which were complementary. These differences in the T_m values were attributed to sheared G:A base pairing[32,33] and a wobble-type base pairing between dG and dT bases.[31]

The results of the fluorescence experiment for the RNA targets were similar to those for the DNA targets. The fluorescence intensities of the duplexes containing the 5′-P-probes were greatest when the discriminating bases were complementary to the target bases, except for the PT/SrG duplex (Fig. 5, right column). The fluorescence of the mismatched PT/SrG duplex was attributed to the wobble-type base pairing between dT and rG bases. Results for the 3′-P-probes are shown in Figure 6 (right column). The fluorescence intensities were greatest when the duplexes were complementary, although the fluorescence intensities of the duplexes composed of the **CP** probe were weak in all target sequences. However, in principle, we could determine the type of nucleobases involved in the SNP sites in the RNA target using four 5′-P-probes or four 3′-P-probes.

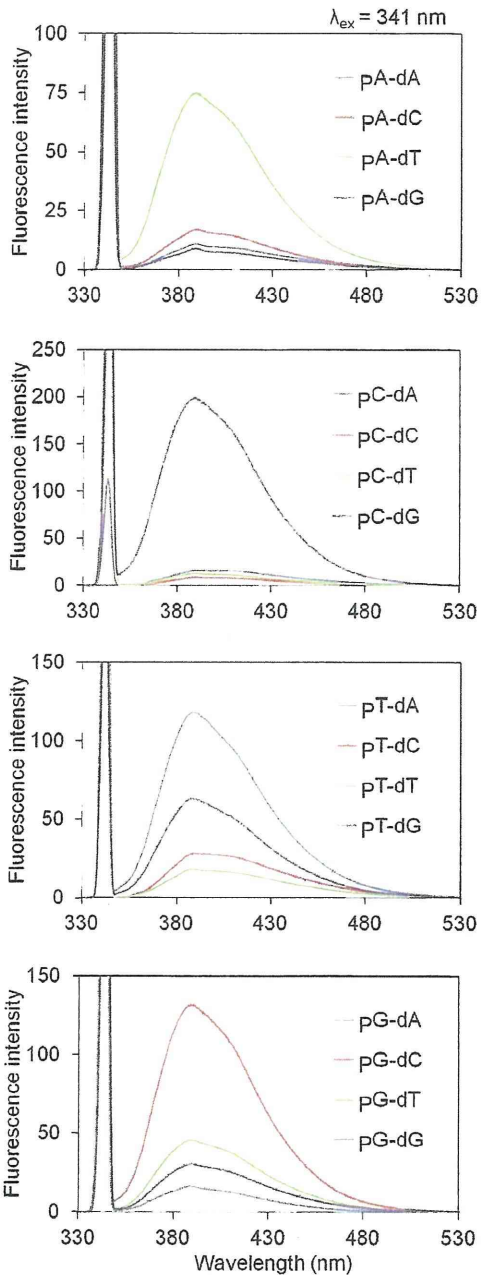

Figure 4. Fluorescence emission spectra of the duplexes. Spectra were obtained under 341-nm excitation on a spectrofluorophotometer in quartz cuvettes with a path length of 1.0 cm and a duplex concentration of 3.0 μM in a T_m buffer at 20 °C. Spectra were recorded with using an excitation slit of 1.5 nm and emission slit of 1.5 nm.

To improve sensitivity and solve the problem related to wobble-type base pairing, we designed and synthesized a probe containing 2-thiothymidine (sT) as a discriminating base. Sekine et al. reported that the formation of wobble-type base pairing between dG and dT can be suppressed by introducing a thiocarbonyl group into the 2-position of dT instead of a 2-carbonyl oxygen (Fig. 7).[34]

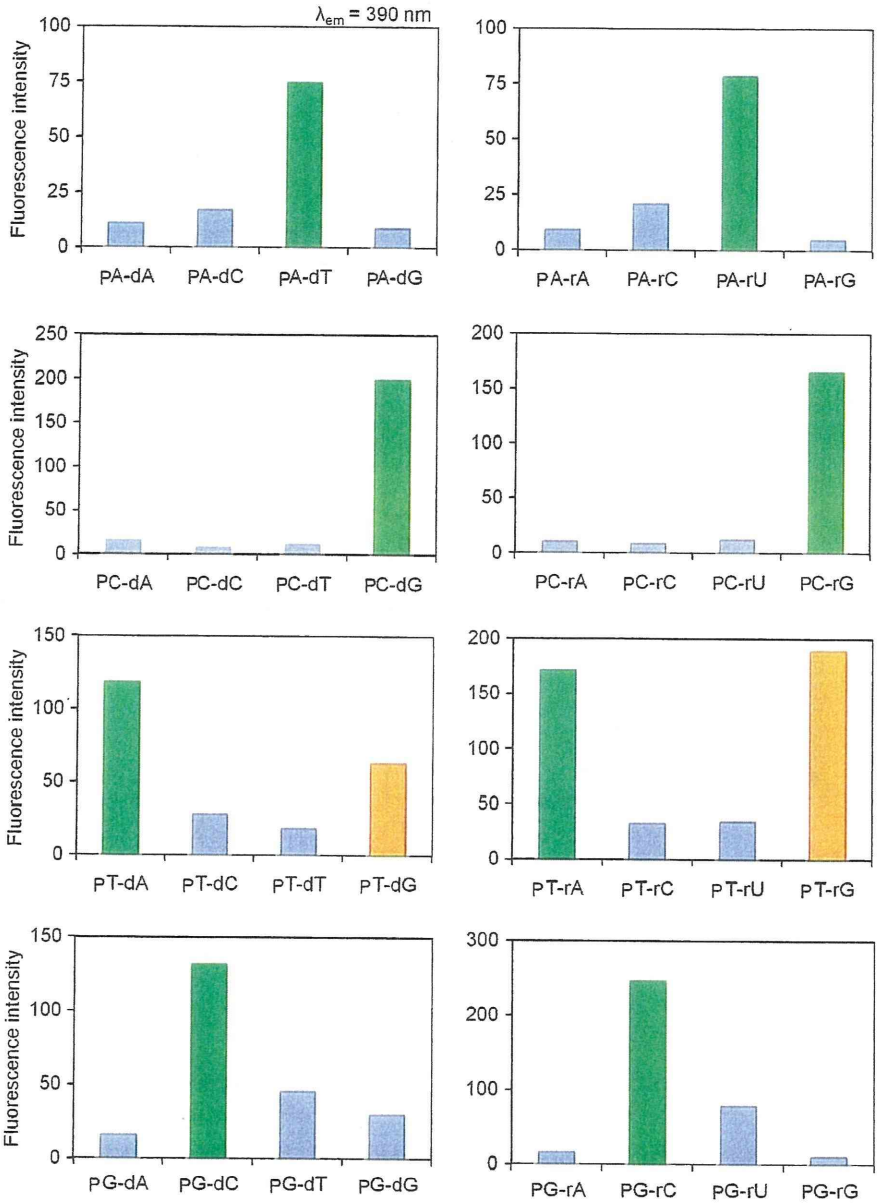

Figure 5. Fluorescence intensities of duplexes at 390 nm. Left column: 5′-P-probe/DNA target. Right column: 5′-P-probe/RNA target. Spectra were measured at 20 °C.

Therefore, we expected that fluorescence due to the formation of wobble-type base pairing could be suppressed by introducing sT instead of dT (Table 2). The results of fluorescence experiments are shown in Fig. 8. The left graph shows the result of the DNA target, while the right graph represents the result of the RNA target. Fluorescence due to the formation of wobble-type base pairing was reduced by introducing sT instead of dT without affecting other base pairings.

3. Discussion and conclusions

A reliable and simple method for detecting nucleotide mutations is very important clinically because sequence variations in human DNA cause genetic diseases and genetically influenced traits. The majority of sequence variations are attributed to SNPs.[1,2] In this study, we developed a novel method for SNP detection. The fluorescence intensity of the nucleoside surrogate **P**, a key compound in this system, depended on solvent polarity. When the probe containing **P** hybridized with a complementary sequence, the probe emitted fluorescence. However, when the probe hybridized with a target containing a mismatched base, the probe did not fluoresce in the almost sequences. Thus, in principle, we can identify the kind of nucleotide involved in an SNP site using 4 probes containing only 1 nucleoside surrogate **P**.

The fluorescence intensity values varied significantly even when the duplex types were the same. For example, the values obtained for the **PA**/SdT and **PC**/SdG duplexes, both of which are successful probes, were 75 and 200, respectively. Similarly, the values obtained for the **PA**/SrU and **PC**/SrG duplexes were 75 and 160. These phenomena may partly reflect the influence of the number of hydrogen bonding between the discriminating bases **D**s and the target bases. The dA:dT base pairing is formed by 2 hydrogen bonds, whereas the base pairing between dG and dC is composed of 3 hydrogen bonds. Thus, when the dG:dC base pair is formed between the discriminating base **D** and the target base, the nucleoside surrogate **P** may flip outside of the DNA helix more largely

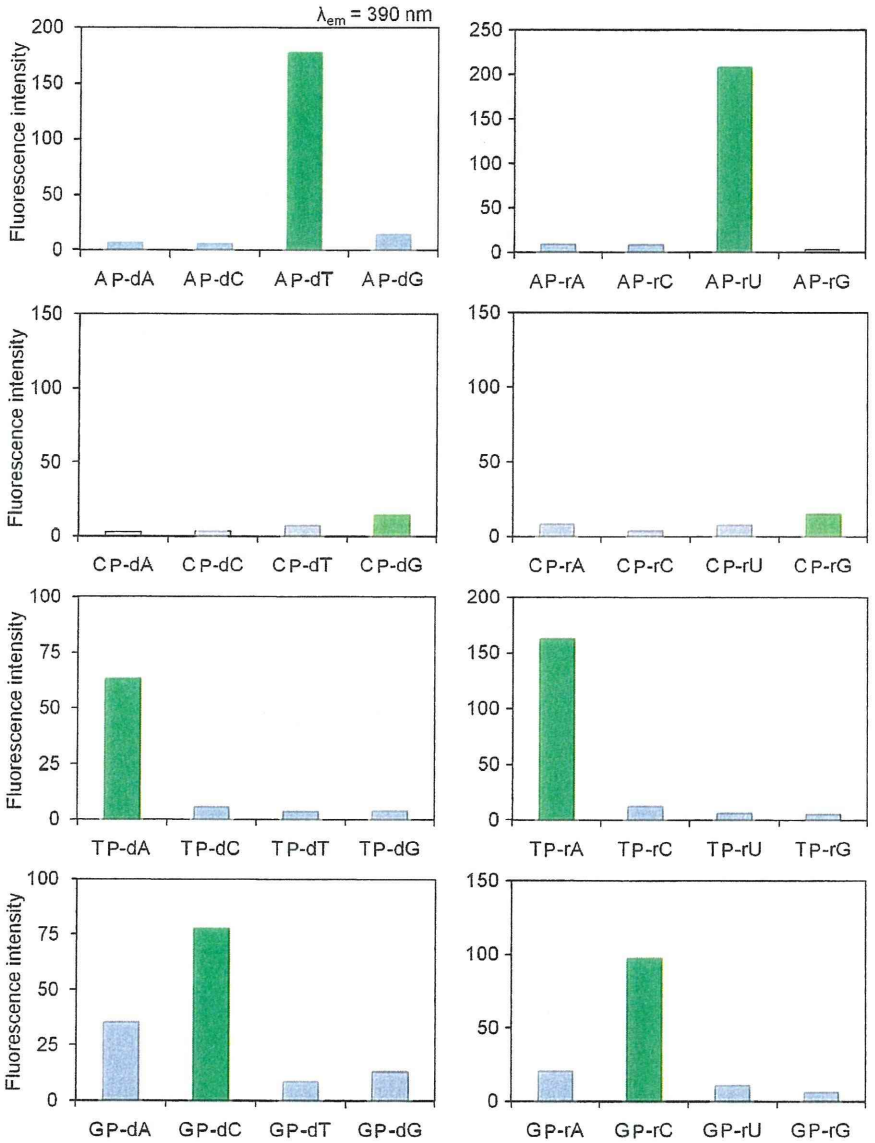

Figure 6. Fluorescence intensities of duplexes at 390 nm. Left column: 3′-P-probe/DNA target. Right column: 3′-P-probe/RNA target. Spectra were measured at 20 °C.

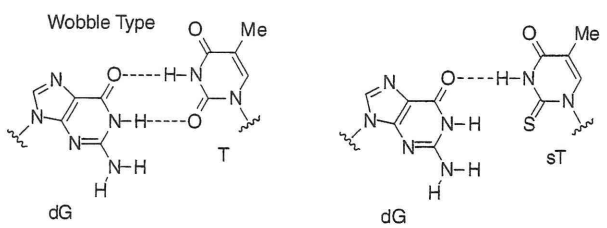

Figure 7. Base pairing between dG and T and between dG and 2-thiothymidine (sT).

as compared with the case of the dA:dT base pair: this may allow the nucleoside surrogate **P** to emit more fluorescence than the case of the dA:dT base pair.

Fluorescence signal patterns of the DNA and RNA target duplexes were not significantly different. Thus, global conformation differences between the duplexes, that is, B-type and A-type conformations, did not influence probe fluorescence intensity. In contrast, the position of the nucleoside surrogate **P** within the probes affected the fluorescence intensity of the duplexes. For example, the **PC** probe (5′-P-probe) worked well for detecting SNPs for the DNA and RNA targets, whereas the **CP** probe (3′-P-probe) did not emit fluorescence even when it hybridized with complementary targets. It is known that a guanine base can form not only a Watson–Crick base pairing with a cytosine base but also a sheared-type base pairing with an adenine base.[32,33] The base moiety of the nucleoside surrogate **P** has a proton donor–acceptor pattern same as adenosine. Thus, the nucleoside surrogate **P** might form a base pairing with the target dG or rG base like as the sheared-type base pairing in the **CP**/SdG or **CP**/SrG duplex. In this study, we tested only one sequence. In the future, we will systematically examine a large number of target sequences to confirm the general applicability of this system.

Fluorescence attributed to wobble-type T:G base pairing was observed for the **PT** probe (5′-P-probe), while the **TP** probe (3′-P-probe) worked well for detecting SNPs for both DNA and RNA targets. These results imply that the geometry of the nucleoside surrogate **P** in the duplexes was different in the 3′-P-probe and

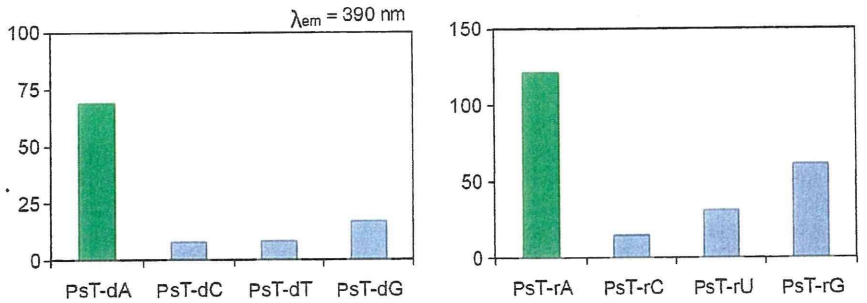

Figure 8. Fluorescence intensities of duplexes containing 2-thiothymidine (sT) at 390 nm. Spectra were measured at 20 °C.

the 5′-P-probe. Furthermore, intensity differences between the fluorescence signals of the matched and mismatched sequences were dependent on the kind of probe and the target sequences. The **AP**, **PC**, and **TP** probes worked well as SNP-detecting probes. When they hybridized with complementary targets, the fluorescence intensities of the duplexes increased 5- to 20-fold as compared to those with mismatched sequences.

As mentioned-above, it is known that a guanine base can form not only a Watson–Crick base pairing with a cytosine base but also a wobble-type base pairing with a thymine base and a sheared-type base pairing with an adenine base.[31–33] In this study, we observed fluorescence signals attributed to wobble-type G:T base pairing. We succeeded in reducing these fluorescence signals by introducing sT instead of dT in the probe. Furthermore, when the **GP** probe hybridized with the SdA target, fluorescence signal intensity increased slightly in comparison to other mismatched targets. This was attributed to sheared-type G:A base pairing. Introducing a chemically modified guanine base might solve the problem and improve the sensitivity of the probe.

In conclusion, we demonstrated the synthesis of DNA containing a fluorescent tricyclic base-linked acyclonucleoside **P**. We examined the properties of the DNA containing **P** as an SNP-detecting probe. We found that, in principle, we can determine the types of nucleobases involved in the SNP sites in DNA and RNA targets with high sensitivities using 4 probes containing **P**. Thus, this system would provide a novel and simple method for detecting SNPs in DNA and RNA targets although we must optimize the linker length and the structure of the base moiety. Synthesis of other fluorescent base-linked acyclonucleosides with distinct emission wavelengths are under investigation in our laboratory.

4. Experimental section

4.1. General remarks

Thin-layer chromatography was carried out on Merck coated plates $60F_{254}$. Silica gel column chromatography was carried out on Wakogel C-300. ^{1}H-, ^{13}C-, and ^{31}P NMR spectra were obtained with a JEOL JNM AL-400 spectrometer. $CDCl_3$ (CIL) or DMSO-d_6 (CIL) was used as a solvent for obtaining NMR spectra. Chemical shifts (δ) are given in parts per million (ppm) downfield from $(CH_3)_4Si$ (δ 0.00 for ^{1}H NMR in $CDCl_3$), 80% H_3PO_4 (δ 0.00 for ^{31}P NMR), or a solvent (for ^{13}C NMR and ^{1}H NMR in DMSO-d_6) as an internal reference with coupling constants (J) in Hz. The abbreviations s, d, and q signify singlet, doublet, and quartet, respectively.

4.1.1. (*S*)-5-Amino-6-cyano-3-[(2,2-dimethyl-1,3-dioxolan-4-yl) methyl]imidazo[4,5-*b*]pyridine (6)

A mixture of (*R*)-2,2-dimethyl-4-(*p*-toluenesulfonyloxymethyl)-1,3-dioxolane (1.70 g, 5.94 mmol), 5-amino-6-cyanoimdazo[4,5-*b*]pyridine (0.76 g, 4.77 mmol),[28] and K_2CO_3 (0.80 g, 5.79 mmol) in DMF (80 mL) was stirred at 60 °C for 70 h. The mixture was partitioned between EtOAc and H_2O. The organic layer was washed with brine, dried (Na_2SO_4), and concentrated. The residue was purified by column chromatography (SiO_2, 1–2% MeOH in $CHCl_3$) to give **6** (0.70 g, 2.56 mmol) in 54% yield: ^{1}H NMR (400 MHz, DMSO-d_6) δ 1.33 (s, 3H, 2-CH_3), 1.38 (s, 3H, 2-CH_3), 3.71 (dd, 1H, J = 6.0 and 8.7, 5-CH_aH$_b$), 4.11 (dd, 1H, J = 6.5 and 8.7, 5-CH$_a$$H_b$), 4.19 (dd, 1H, J = 6.0 and 14.5, NCH_aH$_b$), 4.32 (dd, 1H, J = 3.6 and 14.5, NCH$_a$$H_b$), 4.46 (m, 1H, 4-C*H*), 5.11 (s, 2H, 5-NH_2), 7.97 (s, 1H, 2-*H*), 8.07 (s, 1H, 7-*H*); ^{13}C NMR (100 MHz, DMSO-d_6) δ 24.9, 26.4, 45.0, 65.8, 72.9, 85.3, 108.5, 117.3, 125.9, 133.3, 144.1, 148.6, 156.9; HRMS (FAB) calcd for $C_{13}H_{15}N_5O_2$: 273.1226, found; 273.1229. Anal. Calcd for $C_{13}H_{16}N_6O_2 \cdot 11/50H_2O$: C, 56.32; H, 5.61; N, 25.26. Found: C, 56.58; H, 5.47; N, 24.96.

4.1.2. (*S*)-8-Amino-3-[(2,2-dimethyl-1,3-dioxolan-4-yl) methyl]imidazo[4′,5′:5,6]pyrido[2,3-*d*]pyrimidine (7)

A solution of **6** (1.20 g, 4.39 mmol) in triethyl orthofomate (40 mL, 240 mmol) was stirred at 100 °C for 54 h, cooled to room temperature, and concentrated. The residue was dissolved in saturated NH_3/MeOH (50 mL). The tube was sealed and the solution was stirred at 110 °C for 18 h. After cooling the mixture, the tube was opened and the excess NH_3 was allowed to escape slowly. The mixture was concentrated. The residue was purified by column chromatography (SiO_2, 6–10% MeOH in $CHCl_3$) to give **7** (0.86 g, 2.86 mmol) in 65% yield: ^{1}H NMR (400 MHz, DMSO-d_6) δ 1.22 (s, 3H), 1.27 (s, 3H), 3.82 (dd, 1H, J = 5.1 and 8.7), 4.06 (dd, 1H, J = 6.5 and 8.7), 4.39 (dd, 1H, J = 6.5 and 14.0), 4.47 (dd, 1H, J = 4.2 and 14.0), 4.56 (m, 1H), 7.99 (br s, 2H, D_2O exchangeable), 8.47 (s, 1H), 8.64 (s, 1H), 9.03 (s, 1H); ^{13}C NMR (100 MHz, DMSO-d_6) δ 25.0, 26.5, 45.4, 66.1, 73.3, 91.2, 106.0, 106.9, 109.0, 123.2, 150.3, 151.6, 157.4, 163.9; HRMS (FAB) calcd for $C_{14}H_{17}N_6O_2$: 301.1422, found; 301.1413. Anal. Calcd for $C_{14}H_{17}N_6O_2 \cdot 1/10H_2O$: C, 55.66; H, 5.44; N, 27.82. Found: C, 55.79; H, 5.42; N, 27.50.

4.1.3. (*S*)-8-Amino-3-[2,3-dihydroxypropyl]imidazo[4′,5′:5,6] pyrido[2,3-*d*]pyrimidine (1)

A solution of **7** (0.86 g, 2.86 mmol) in 80% CH_3CO_2H (30 mL) was stirred at 60 °C for 9 h. The solvent was evaporated in vacuo to give **1** (0.74 g, 2.83 mmol) in 98% yield: UV λ_{max} (H_2O) 260 nm (ε = 14700), 333 nm (ε = 18300); ^{1}H NMR (400 MHz, DMSO-d_6) δ 3.39 (m, 2H), 3.93 (m, 1H), 4.14 (dd, 1H, J = 8.7 and 13.9), 4.48 (dd, 1H, J = 3.4 and 14.0), 4.90 (t, 1H, J = 5.5), 5.14 (d, 1H, J = 5.9), 7.97 (br s, 2H), 8.47 (s, 1H), 8.59 (s, 1H), 9.01 (s, 1H); ^{13}C NMR (100 MHz, DMSO-d_6) δ 46.6, 63.7, 69.3, 105.8, 122.9, 134.0, 150.7, 151.6, 155.1, 157.3, 163.9; HRMS (FAB) calcd for $C_{11}H_{13}N_6O_2$: 261.1111, found; 261.1100. Anal. Calcd for $C_{11}H_{13}N_6O_2 \cdot 1/5$ H_2O: C, 50.29; H, 4.74; N, 30.87. Found: C, 50.37; H, 4.87; N, 30.89.

4.1.4. (*S*)-8-Amino-3-[2,3-bis(*tert*-butyldimethylsilyloxy) propyl]imidazo[4′,5′:5,6]pyrido[2,3-*d*]pyrimidine (8)

A solution of **1** (0.75 g, 2.88 mmol), imidazole (1.75 g, 25.7 mmol), TBDMSCl (1.58 g, 10.5 mmol) in DMF (30 mL) was stirred at room temperature for 18 h. EtOH (1 mL) was added to the mixture, and the whole was stirred for 10 min. The mixture was partitioned between EtOAc and H_2O. The organic layer was washed with aqueous $NaHCO_3$ (saturated) and brine, dried (Na_2SO_4), and concentrated. The residue was purified by column chromatography (SiO_2, 3% MeOH in $CHCl_3$) to give **8** (1.14 g, 2.33 mmol) in 81% yield: ^{1}H NMR (400 MHz, DMSO-d_6) δ −0.63 (s, 3H), −0.15 (s, 3H), 0.08 (s, 6H), 0.65 (s, 9H), 0.90 (s, 9H), 3.66 (m, 2H), 4.26 (m, 2H), 4.47 (m, 1H), 7.98 (br s, 2H), 8.47 (s, 1H), 8.58 (s, 1H), 9.01 (s, 1H); ^{13}C NMR (100 MHz, DMSO-d_6) δ −5.9, −5.5, −5.4, −4.9, 17.4, 18.1, 25.5, 25.9, 46.7, 65.7, 70.4, 105.8, 123.0, 134.1, 150.6, 151.6, 155.2, 157.3, 163.9; HRMS (FAB) calcd for $C_{23}H_{40}N_6O_2Si_2$: 488.2751, found; 488.2760. Anal. Calcd for $C_{23}H_{40}N_6O_2Si_2$: C, 56.52; H, 8.25; N, 17.19. Found: C, 56.37; H, 8.10; N, 17.24.

4.1.5. (*S*)-N^8-Benzoylamino-3-[2,3-bis(*tert*-butyldimethylsilyl oxy)propyl]imidazo[4′,5′:5,6]pyrido[2,3-*d*]pyrimidine (9)

A solution of **8** (1.82 g, 3.72 mmol) and BzCl (0.64 mL, 5.51 mmol) in pyridine (20 mL) was stirred at room temperature. After 10 h, the mixture was partitioned between $CHCl_3$ and H_2O. The organic layer was washed with aqueous $NaHCO_3$ (saturated) and brine, dried (Na_2SO_4), and concentrated. The residue was purified by column chromatography (SiO_2, 0–10% MeOH in $CHCl_3$) to give **9** (1.48 g, 2.50 mmol) in 67% yield: ^{1}H NMR (400 MHz, $CDCl_3$) δ −0.47 (s, 3H), −0.08 (s, 3H), 0.07 (s, 6H), 0.78 (s, 9H), 0.92 (s, 9H), 3.61 (m, 1H), 3.70 (m, 1H), 4.23 (m, 1H), 4.37 (m, 1H), 4.67 (m, 1H), 7.51–7.57 (m, 3H), 8.37–8.48 (m, 4H), 9.53 (s, 1H); ^{13}C NMR (100 MHz, $CDCl_3$) δ −5.4, −5.3, −4.7, 17.8, 18.4, 25.7, 26.0, 47.4, 65.4, 70.7, 113.6, 126.9, 128.3, 130.0, 132.7, 135.9, 137.2, 143.6, 150.6, 152.6, 154.2, 159.0, 180.0. Anal. Calcd for $C_{23}H_{44}N_6O_3Si_2$: C, 60.77; H, 7.48; N, 14.09. Found: C, 60.51.; H, 7.40; N, 14.11.

4.1.6. (*S*)-N^8-Benzoylamino-3-[2,3-dihydroxypropyl]imidazo[4′, 5′:5,6]pyrido[2,3-*d*]pyrimidine (10)

A solution of **9** (1.48 g, 2.50 mmol) and TBAF (9.96 mL, 9.96 mmol, 1 M THF solution) in THF (50 mL) was stirred at room temperature. After 2 h, the solvent was evaporated in vacuo. The residue was purified by column chromatography (SiO_2, 5–14% MeOH in $CHCl_3$) to give **10** (0.68 g, 1.87 mmol) in 75% yield: ^{1}H NMR (400 MHz, DMSO-d_6) δ 3.41 (ddd, 1H, J = 5.5, 5.5 and 11.0), 3.48 (ddd, 1H, J = 5.5, 5.5 and 11.0), 3.97 (m, 1H), 4.21 (dd, 1H, J = 8.8 and 14.0), 4.55 (dd, 1H, J = 3.4 and 14.0), 4.92 (t, 1H, J = 5.5), 5.18 (d, 1H, J = 5.5), 7.54–8.38 (m, 7H), 8.76 (s, 1H); ^{13}C NMR (100 MHz, DMSO-d_6) δ 47.4, 64.3, 69.8, 125.6, 128.9, 129.7, 132.7 (multiple), 135.7 (multiple), 152.8; HRMS (FAB) calcd for $C_{18}H_{16}N_6O_3$: 365.1362, found; 365.1361. Anal. Calcd for $C_{18}H_{67}N_6O_3 \cdot 7/10H_2O$: C, 57.35; H, 4.65; N, 22.29. Found: C, 57.45; H, 4.73; N, 22.08.

4.1.7. (*S*)-N^8-Benzoylamino-3-[3-(4,4′-dimethoxytrityloxy)-2-hydroxypropyl]imidazo[4′,5′:5,6]pyrido[2,3-*d*]pyrimidine (11)

A solution of **10** (0.60 g, 1.65 mmol) and DMTrCl (0.84 g, 2.48 mmol) in pyridine (6 mL) was stirred at room temperature. After 2 h, the mixture was partitioned between $CHCl_3$ and H_2O. The organic layer was washed with aqueous $NaHCO_3$ (saturated) and brine, dried (Na_2SO_4), and concentrated. The residue was purified by column chromatography (SiO_2, 1% MeOH in $CHCl_3$) to give **11** (0.62 g, 0.93 mmol) in 56% yield: ^{1}H NMR (400 MHz, $CDCl_3$) δ 3.09 (m, 1H), 3.17 (dd, 1H, J = 6.3 and 9.9), 3.31 (dd, 1H, J = 4.4 and 9.9), 4.29 (m, 1H), 4.42 (dd, 1H, J = 7.5 and 14.4), 4.63 (dd, 1H, J = 3.2 and 14.4), 6.08–6.82 (m, 4H), 7.22–7.31 (m, 7H), 7.34–7.41 (m, 2H), 7.51–7.60 (m, 3H), 8.40 (m, 2H), 8.48 (m, 2H), 9.52 (s, 1H); ^{13}C NMR (100 MHz, $CDCl_3$) δ 47.6, 55.3, 64.9, 69.0, 86.6, 113.3, 126.4, 127.1, 127.3, 128.0, 128.1, 128.4, 130.0, 130.1, 132.7, 135.4, 135.6, 135.7, 144.6, 150.5, 152.3, 158.7. Anal. Calcd for $C_{39}H_{34}N_6O_5 \cdot 9/5H_2O$: C, 67.00; H, 5.42; N, 12.02. Found: C, 67.34; H, 5.08; N, 11.63.

4.1.8. N^8-Benzoylamino-3-[(*R*)-3-(4,4′-dimethoxytrityloxy) -2-[[(2-cyanoethoxy)(*N*,*N*-diisopropylamino)phosphanyl]oxy] -propyl]imidazo[4′,5′:5,6]pyrido[2,3-*d*]pyrimidine (12)

A solution of 11 (0.50 g, 0.75 mmol), *N*,*N*-diisopropylethylamine (0.65 mL, 3.74 mmol), and chloro(2-cyanoethoxy)(*N*,*N*-diisopropylamino)phosphine (0.33 mL, 1.48 mmol) in THF (4 mL) was stirred at room temperature. After 30 min, the mixture was partitioned between $CHCl_3$ and H_2O. The organic layer was washed with aqueous $NaHCO_3$ (saturated) and brine, dried (Na_2SO_4), and concentrated. The residue was purified by column chromatography (SiO_2, 50% EtOAc in hexane) to give **12** (0.43 g, 0.50 mmol) in 67% yield: ^{31}P NMR (162 MHz, DMSO-d_6) δ 149.1, 150.2.

4.2. Oligonucleotide synthesis

The synthesis was carried out with a DNA/RNA synthesizer (Applied Biosystems Model 3400) by the phosphoramidite method. In the case of the coupling of the amidite **12**, a 0.12 M solution of the amidite **12** in CH_3CN and a coupling time of 15 min were used. Deprotection of the bases and phosphates was performed in concentrated NH_4OH at 55 °C for 16 h. The oligonucleotides were purified by 20% PAGE containing 7 M urea to give the highly purified oligonucleotides, **PA** (14), **PG** (40), **PC** (20), **PT** (8), **AP** (15), **GP** (15), **CP** (14), **TP** (29), and **PsT** (15). The yields are indicated in parentheses as OD units at 260 nm starting from 1.0 μmol scale. The extinction coefficients of the oligonucleotides were calculated from those of mononucleotides and dinucleotides according to the nearest-neighbor approximation method.[35]

4.3. MALDI-TOF/MS analyses of oligonucleotides

Spectra were obtained with a SHIMADZU AXIMA-CFR plus time-of-flight mass spectrometer equipped with a nitrogen laser (337 nm, 3-ns pulse). A solution of 3-hydroxypicolinic acid (3-HPA) and diammonium hydrogen citrate in H_2O was used as the matrix. **PA**: calculated mass, 5844.8; observed mass, 5846.2. **PG**: calculated mass, 5860.8; observed mass, 5856.2. **PC**: calculated mass, 5820.8; observed mass, 5823.8. **PT**: calculated mass, 5835.8; observed mass, 5833.0. **AP**: calculated mass, 5844.8; observed mass, 5843.6. **GP**: calculated mass, 5860.8; observed mass, 5862.2. **CP**: calculated mass, 5820.8; observed mass, 5823.0. **TP**: calculated mass, 5835.8; observed mass, 5837.1. **PsT**: calculated mass, 5851.7; observed mass, 5851.1.

4.4. Absorption experiments

Absorption spectra (200–500 nm) were obtained on a SHIMAZU UV-2450 UV–Vis spectrophotometer in quartz cuvettes with a path length of 1.0 cm and a 30 μM **P** concentration in an appropriate solvent.

4.5. Thermal denaturation study

The solution containing the duplex in a buffer comprising 10 mM sodium phosphate (pH 7.0) and 0.1 M NaCl was heated at 95 °C for 3 min, cooled gradually to an appropriate temperature, and then used for the thermal denaturation study. The thermal-induced transition of each mixture was monitored at 260 nm on a SHIMAZU UV-2450 UV–Vis spectrophotometer fitted with a temperature controller in quartz cuvettes with a path length of

1.0 cm and a 3.0 μM duplex concentration in a buffer of 10 mM sodium phosphate (pH 7.0) and 0.1 M NaCl. The sample temperature was increased by 0.5 °C/min.

4.6. Fluorescence experiments

Steady-state fluorescence emission spectra (370–670 nm) were obtained on a SHIMADZU RF-5300PC spectrofluorophotometer in quartz cuvettes with a path length of 1.0 cm and a 30 μM **P** concentration in an appropriate solvent or a 3.0 μM duplex concentration in a T_m buffer at 20 °C. Spectra were recorded with use of excitation slit of 1.5 nm and emission slit of 1.5 nm for **P** or excitation slit of 3.0 nm and emission slit of 3.0 nm for the duplexes. The fluorescence quantum yield (Φ_{em}) was determined by use of quinine as a reference with the known Φ_{em} value of 0.58 (22 °C) in 0.1 M H_2SO_4. The quantum yield was calculated according to the following equation: $\Phi_{em(S)}/\Phi_{em(R)} = (I_{(S)}/I_{(R)}) \times (A_{(S)}/A_{(R)}) \times (n_{(S)}{}^2/n_{(R)}{}^2)$. Here, $\Phi_{em(S)}$ and $\Phi_{em(R)}$ are the fluorescence quantum yields of the sample and the reference, respectively, $I_{(S)}$ and $I_{(R)}$ are the integrated fluorescence intensities of the sample and the reference, respectively, $A_{(S)}$ and $A_{(R)}$ are the respective optical density of the sample and the reference solutions at the wavelength of excitation, and $n_{(S)}{}^2$ and $n_{(R)}{}^2$ are the values of the refractive index for the respective solvents.

Acknowledgments

This study was supported in part by a Grant-in-Aid from Precursory Research for Embryonic Science and Technology (PRESTO) of Japan Science and Technology (JST), a Grant-in-Aid from the Koshiyama Research Grand and a Grant-in-Aid for Scientific Research (C) from the Japan Society for the Promotion of Science (JSPS) to Y.U.

Supplementary data

Supplementary data associated with this article can be found, in the online version, at doi:10.1016/j.bmc.2011.11.045.

References and notes

1. Sachidanandam, R.; Weissman, D.; Schmidt, S. C.; Kakol, J. M.; Stein, L. D.; Marth, G.; Sherry, S.; Mullikin, J. C.; Mortimore, B. J.; Willey, D. L., et al *Nature* **2001**, *409*, 928.
2. Venter, J. C.; Adams, M. D.; Myers, E. W.; Li, P. W.; Mural, R. J.; Sutton, G. G.; Smith, H. O.; Yandell, M.; Evans, C. A.; Holt, R. A., et al *Science* **2001**, *291*, 1304.
3. McCarthy, J. J.; Hilfiker, R. *Nat. Biotechnol.* **2000**, *18*, 505.
4. Wang, D. G.; Fan, J.-B.; Siao, C.-J.; Berno, A.; Young, P.; Sapolsky, R.; Ghandour, G.; Perkins, N.; Winchester, E.; Spencer, J., et al *Science* **1998**, *280*, 1077.
5. Hoheisel, J. D. *Nat. Rev. Genet.* **2006**, *7*, 200.
6. Hardenbol, P.; Baner, J.; Jain, M.; Nilsson, M.; Namsaraev, E. A.; Karlin-Neumann, G. A.; Fakhrai-Rad, H.; Ronaghi, M.; Willis, T. D.; Landegren, U.; Davis, R. W. *Nat. Biotechnol.* **2003**, *21*, 673.
7. Holland, P. M.; Abramson, R. D.; Watson, R.; Gelfand, D. H. *Proc. Natl. Acad. Sci. U.S.A.* **1991**, *88*, 7276.
8. Pourmand, N.; Elahi, E.; Davis, R. W.; Ronaghi, M. *Nucleic Acids Res.* **2002**, *30*, e31.
9. Lindroos, K.; Liljedahl, U.; Raitio, M.; Syvanen, A.-C. *Nucleic Acids Res.* **2001**, *29*, e69.
10. Ross, P.; Hall, L.; Smirnov, I.; Haff, L. *Nat. Biotechnol.* **1998**, *16*, 1347.
11. Stoerker, J.; Mayo, J. D.; Tetzlaff, C. N.; Sarracino, D. A.; Schwope, I.; Richert, C. *Nat. Biotechnol.* **2000**, *18*, 1213.
12. Okamoto, A.; Tanaka, K.; Saito, I. *J. Am. Chem. Soc.* **2003**, *125*, 4972.
13. Okamoto, A.; Tanaka, K.; Fukuta, T.; Saito, I. *J. Am. Chem. Soc.* **2003**, *125*, 9296.
14. Okamoto, A.; Kanatani, K.; Saito, I. *J. Am. Chem. Soc.* **2004**, *126*, 4820.
15. Saito, Y.; Hanawa, K.; Motegi, K.; Omoto, K.; Okamoto, A.; Saito, I. *Tetrahedron Lett.* **2005**, *46*, 7605.
16. Okamoto, A.; Tainaka, K.; Unzai, T.; Saito, I. *Tetrahedron* **2007**, *63*, 3465.
17. Tainaka, K.; Tanaka, K.; Ikeda, S.; Nishiza, K.; Unzai, T.; Fujiwara, Y.; Saito, I.; Okamoto, A. *J. Am. Chem. Soc.* **2007**, *129*, 4776.
18. Köhler, O.; Seitz, O. *Chem. Commun.* **2003**, 2938.
19. Köhler, O.; Jarikote, D. V.; Seitz, O. *ChemBioChem* **2005**, *6*, 69.
20. Jarikote, D. V.; Krebs, N.; Tannert, S.; Röder, B.; Seitz, O. *Chem. Eur. J.* **2007**, *13*, 300.
21. Bethge, L.; Jarikote, D. V.; Seitz, O. *Bioorg. Med. Chem.* **2008**, *16*, 114.
22. Bethge, L.; Singh, I.; Seitz, O. *Org. Biomol. Chem.* **2010**, *8*, 2439.
23. Young, M. A.; Jayaram, B.; Beveridge, D. L. *J. Phys. Chem. B* **1998**, *102*, 7666.
24. Dvorakova, H.; Holy, A.; Masojidkova, M. *Collect. Czech. Chem. Commun.* **1988**, *53*, 1779.
25. Clayton, R.; Davis, M. L.; Fraser, W.; Li, W.; Ramsden, C. A. *Synlett* **2002**, 1483.
26. Liu, H.; Gao, J.; Lynch, S. R.; Saito, Y. D.; Maynard, L.; Kool, E. T. *Science* **2003**, *302*, 868.
27. Liu, H.; Gao, J.; Maynard, L.; Saito, Y. D.; Kool, E. T. *J. Am. Chem. Soc.* **2004**, *126*, 1102.
28. Harris, P. A.; Pendergast, W. *J. Heterocycl. Chem.* **1996**, *33*, 319.
29. Rettie, A. E.; Wienkers, L. C.; Gonzalez, F. J.; Trager, W. F.; Korzekwa, K. R. *Pharmacogenetics* **1994**, *4*, 39.
30. Sullivan-Klose, T. H.; Ghanayem, B. I.; Bell, D. A.; Zhang, Z.-Y.; Kaminsky, L. S.; Shenfield, G. M.; Miners, J. O.; Birkett, D. J.; Goldstein, J. A. *Pharmacogenetics* **1996**, *6*, 341.
31. Hunter, W. N.; Kneale, G.; Brown, T.; Rabinovich, D.; Kennard, O. *J. Mol. Biol.* **1986**, *190*, 605.
32. Gao, Y.-G.; Robinson, H.; Sanishvili, R.; Joachimiak, A.; Wang, A. H.-J. *Biochemistry* **1999**, *38*, 16452.
33. Sargueil, B.; McKenna, J.; Burke, J. M. *J. Biol. Chem.* **2000**, *275*, 32157.
34. Okamoto, I.; Shohda, K.; Seio, K.; Sekine, M. *J. Org. Chem.* **2003**, *68*, 9971.
35. Puglisi, J. D.; Tinoco, I. In *Methods in Enzymology*; Dahlberg, J. E., Abelson, J. N., Eds.; Academic Press: San Diego, 1989; Vol. 180, pp 304–325.

Bioorganic & Medicinal Chemistry Letters 22 (2012) 2681–2683

Contents lists available at SciVerse ScienceDirect

Bioorganic & Medicinal Chemistry Letters

journal homepage: www.elsevier.com/locate/bmcl

Double-stranded oligonucleotides containing 5-aminomethyl-2′-deoxyuridine form thermostable anti-parallel triplexes with single-stranded DNA or RNA

Aya Shibata [a], Yoshihito Ueno [b,*], Mari Iwata [a], Haruka Wakita [a], Akira Matsuda [c], Yukio Kitade [a]

[a] Department of Biomolecular Science, Faculty of Engineering, Gifu University, Yanagido, Gifu 501-1193, Japan
[b] Department of Applied Life Science, Faculty of Applied Biological Sciences, Gifu University, Yanagido, Gifu 501-1193, Japan
[c] Graduate School of Pharmaceutical Sciences, Hokkaido University, Kita-12, Nishi-6, Kita-ku, Sapporo 060-0812, Japan

ARTICLE INFO

Article history:
Available online 14 March 2012

Keywords:
DNA
RNA
Triplex
Antisense
Aminoalkyl linker
Thermal stability

ABSTRACT

This Letter describes the synthesis and properties of double-stranded antisense oligonucleotides connected with a pentaerythritol linker. We found that double-stranded antisense oligonucleotides with aminomethyl residues have high affinity for single-stranded DNA or RNA in buffer solutions with and without $MgCl_2$. Thus, these oligonucleotides would be useful as antisense oligonucleotides for targeting single-stranded RNA through triplex formation.

Thanks to the discovery of a large number of non-coding RNAs, gene suppression by using antisense oligonucleotides has once again attracted much attention.[1–3] An antisense oligonucleotide binds to the target mRNA via Watson–Crick hydrogen bonds, whereas an antigene oligonucleotide binds to the major groove of double-stranded DNA by Hoogsteen or reverse Hoogsteen hydrogen bonds and forms a local triple helix (triplex).[4] Recently, we reported an approach whereby single-stranded DNA or RNA is targeted through triplex formation by using a branched oligonucleotide.[5–7]

Approaches using branched oligonucleotides can be classified into 2 categories based on the orientation of the triplexes: one method utilizes parallel triplexes, in which the third strand binds to the second strand via Hoogsteen hydrogen bonds (Fig. 1a), whereas the other method utilizes antiparallel triplexes, where the third strand binds to the second strand via reverse Hoogsteen hydrogen bonds (Fig. 1b). In a previous report, we described the synthesis of double-stranded antisense oligonucleotides connected with a pentaerythritol linker that could target single-stranded DNA or RNA by forming parallel triplexes.[5–7] It was found that the double-stranded oligonucleotides formed more thermally stable triplexes than the corresponding Watson–Crick duplex with a single-stranded RNA.[6,7] This suggests that the double-stranded oligonucleotides are useful as an antisense oligonucleotide. In this Letter, we describe the synthesis and properties of double-stranded antisense oligonucleotides that can target single-stranded DNA or RNA by forming antiparallel triplexes.

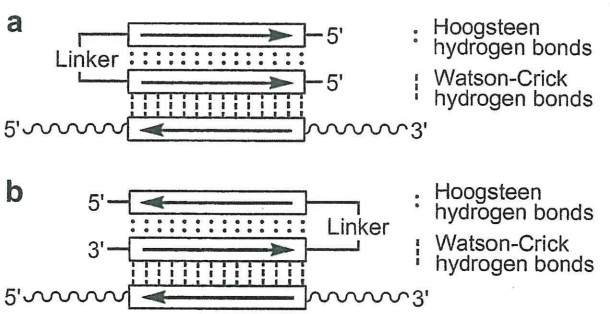

Figure 1. Schematic representation of branched oligonucleotides binding to single-stranded nucleic acids.

Thus far, oligonucleotide analogs carrying various polyamines have been synthesized,[8–14] and some of them have been shown to increase the thermal stability of duplexes and parallel triplexes. However, to the best of our knowledge, the stabilization effects of aminoalkyl modifications on antiparallel triplex formation have not been examined. X-ray crystal structure analysis of antiparallel triplexes showed that the 5-position of the thymidine residues of the third strand is positioned very close to the phosphate backbone

* Corresponding author. Tel./fax: +81 58 293 2919.
E-mail address: uenoy@gifu-u.ac.jp (Y. Ueno).

0960-894X/$ - see front matter © 2012 Elsevier Ltd. All rights reserved.
http://dx.doi.org/10.1016/j.bmcl.2012.03.024

target duplex

II 3'-d(GAGGAGGGAGGA)-5'

I 5'-d(CTCCTCCCTCCT)-3'

Z =

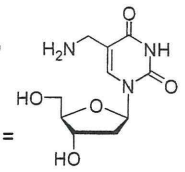

	3rd strand	K_d (nM)
III	5'-d(GTGGTGGGTGGT)-3'	115 ± 9
IV	5'-d(GTGGTGGGZGGT)-3'	128 ± 19
V	5'-d(GTGGZGGGZGGT)-3'	82 ± 4
VI	5'-d(GZGGZGGGZGGT)-3'	48 ± 6
VII	5'-d(GZGGZGGGZGGZ)-3'	68 ± 4

Figure 2. Binding abilities of the oligonucleotides for the target duplex.

of the second strand.[15] Thus, we hypothesized that introduction of an aminomethyl residue into the 5-position of the 2′-deoxyuridine in the third strand would increase the thermal stability of the antiparallel triplex because the ammonium cations of the aminomethyl residues would reduce the anionic electrostatic repulsion between the phosphate moieties.

Oligonucleotides containing 5-aminomethyl-2′-deoxyuridine (**Z**) were synthesized using the phosphoramidite method (Fig. 2). The synthetic route of a **Z** phosphoramidite is shown in Figure S1. All **Z**-containing oligonucleotides were synthesized using a DNA/RNA synthesizer. The obtained oligonucleotides were analyzed using matrix-assisted laser desorption/ionization time-of-flight mass spectrometry (MALDI-TOF/MS), and the observed molecular weights were in agreement with their structures.

First, binding of the aminomethyl-modified oligonucleotides to target DNA was examined using an electrophoretic mobility shift assay (EMSA). Figure 2 summarizes the dissociation constants (K_d) of the third strands bound to the duplex DNA target. The K_d of the unmodified third strand, **III**, to the target DNA was 115 ± 9 nM, whereas those of the third strands **V**, **VI**, and **VII** containing 2, 3, and 4 **Z** residues were 82 ± 4, 48 ± 6, and 68 ± 4 nM, respectively. Thus, this proved that the aminomethyl modification at the 5-position of the 2′-deoxyuridine in the third strand increases the stability of the antiparallel triplex. The K_d (128 ± 19 nM) of the third strand, **IV**, containing 1 **Z** residue was slightly lower than that of the unmodified third strand, **III**. Thus, plural **Z** residues seemed to be required for the triplex stabilization.

Branched oligonucleotides **IX** and **X** were synthesized using an appropriately protected pentaerythritol linker (Fig. 3). The stability of triplexes formed with these oligonucleotides was studied by thermal denaturation in Tris–HCl buffer solution (15 mM, pH 7.0) containing 25 mM NaCl and 5 mM $MgCl_2$ (Figs. 3 and S2). One transition was observed in the melting profile when branched oligonucleotide **IX** and single-stranded RNA **VIII** were used, and the melting temperature (T_m) was 67.6 °C. In contrast, the T_m of the duplex between single-stranded DNA **II** and RNA **VIII** was 54.5 °C. The increment in the absorbance melting curve of the **VIII**:**IX** complex was greater than that of the **VIII**:**II** duplex. This means that thermal denaturation from triplex to complete random coil for the **VIII**:**IX** complex occurred cooperatively in a single transition. On the other hand, the **VIII**:**II**:**III** triplex did not show a clear T_m transition, that might be due to aggregation of the oligonucleotide strands containing many guanine residues. Thus, it turned out that the oligonucleotide **IX** connected with the pentaerythritol linker forms a more thermostable triplex with the single-stranded RNA **VIII** than the corresponding **VIII**:**II** duplex. We also performed a thermal denaturation study with target RNA that contained one base mismatch (Fig. S3). The ΔT_m (T_m [a complex between an oligonucleotide and a complementary target] − T_m [a complex between an oligonucleotide and a target containing a mismatched base]) ranged from −7.2 to −12.4 °C. Thus, it was found that the branched oligonucleotide **IX** has sufficient base discrimination ability as an antisense oligonucleotide. Incorporation of 3 aminomethyl residues into the branched oligonucleotide slightly stabilized the triplex in the buffer solution containing $MgCl_2$. The ΔT_m between the triplexes **VIII**:**X** and **VIII**:**IX** was +2.7 °C. Similar phenomena were observed when single-stranded DNA **I** was used as the target (Fig. 3, top graph).

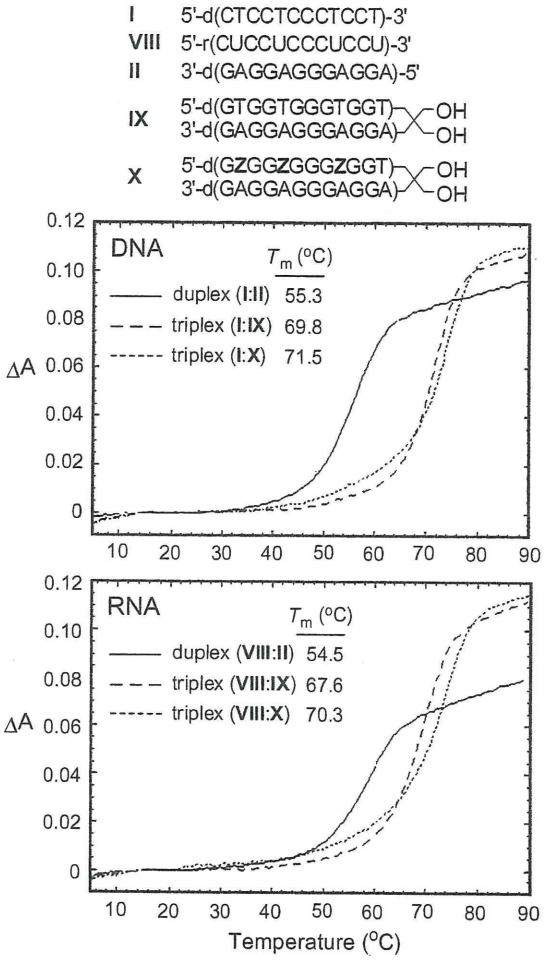

Figure 3. UV melting profiles. Melting experiments were performed in Tris–HCl buffer solution (15 mM, pH 7.0) containing 25 mM NaCl and 5.0 mM $MgCl_2$. The concentrations of the complexes were 2.0 μM.

It was reported that divalent cations, such as Mg^{2+}, are necessary for the formation of an antiparallel triplex.[16,17] Next, we demonstrated thermal denaturation in a buffer solution that did not contain $MgCl_2$. As shown in Fig. S2, the T_m of the complexes **I**:**IX**, **I**:**X**, **VIII**:**IX**, and **VIII**:**X** were significantly decreased. The T_m of the complexes were almost equal to those of the corresponding **I**:**II** and **VIII**:**II** duplexes. However, intriguingly, the increment in the absorbance melting curves of the **VIII**:**X** complex was greater than that of the **VIII**:**II** duplex. This suggested that the aminomethyl residue-containing branched oligonucleotide **X** formed an antiparallel triplex with the single-stranded RNA **VIII** in the absence of Mg^{2+}. The circular dichroism spectrum demonstrated not only triplex formation between the branched oligonucleotide **X** and the target RNA **VIII** but also triplex formation between the

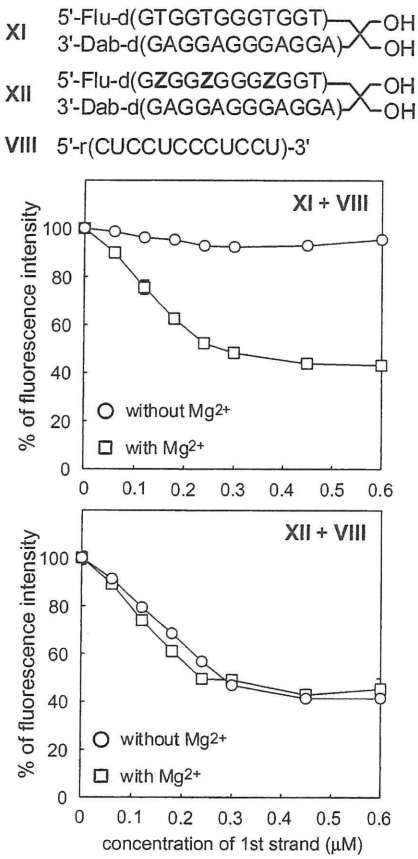

Figure 4. Profiles of the fluorescence intensities versus the first strand concentrations. Experiments were performed in Tris–HCl buffer solution (15 mM, pH 7.0) containing 25 mM NaCl in the presence or absence of 5.0 mM $MgCl_2$. The concentrations of the labeled oligonucleotides (**XI** and **XII**) were 0.30 μM. Excitation wavelength: 485 nm. Emission wavelength: 535 nm.

branched oligonucleotide **X** and the target DNA **I** in the absence of Mg^{2+} (Fig. S4).

In order to confirm the formation of the triplex, we next performed fluorescence resonance energy transfer (FRET) analysis. For this, we synthesized the branched oligonucleotides **XI** and **XII**, which were modified with fluorescein (Flu) at the 5′-end and with dabcyl (Dab) at the 3′-end as a quencher (Fig. 4). When the branched oligonucleotide **XI** was mixed with the target RNA **VIII** in the absence of Mg^{2+}, the fluorescence intensities of the solutions were almost the same irrespective of the concentrations of the first strand **VIII** (Fig. 4, top graph). On the other hand, the fluorescence intensities of the solutions decreased as the concentrations of the first strand **VIII** increased, and plateaued at a 1:1 branched oligonucleotide **XI** and first strand **VIII** ratio when the branched oligonucleotide **XI** was mixed with the target RNA **VIII** in the presence of Mg^{2+}. This indicates that the branched oligonucleotide **XI** forms a triplex with the target RNA **VIII** in the presence of Mg^{2+} but not in the absence of Mg^{2+}.

When the branched oligonucleotide **XII** containing the aminomethyl residues was used, the fluorescence intensities of the solutions decreased as the concentrations of the first strand **VIII** increased even in the absence of Mg^{2+}, and plateaued near a 1:1 branched oligonucleotide **XII** and first strand **VIII** ratio (Fig. 4, bottom graph). This proved that the branched oligonucleotide **XII**, which is modified with the aminomethyl residues, could form an antiparallel triplex even in the absence of a divalent cation such as Mg^{2+}.

In conclusion, we have demonstrated the synthesis of branched oligonucleotides containing aminomethyl residues, and found that these oligonucleotides have a high affinity for single-stranded DNA or RNA in buffer solutions with and without $MgCl_2$. Thus, these oligonucleotides would be useful as antisense oligonucleotides for targeting single-stranded RNA through triplex formation.

Acknowledgments

This study was supported in part by a Grant-in-Aid from the Koshiyama Research Grand and a Grant-in-Aid for Scientific Research (C) from the Japan Society for the Promotion of Science to Y.U.

Supplementary data

Supplementary data associated with this article can be found, in the online version, at http://dx.doi.org/10.1016/j.bmcl.2012.03.024.

References and notes

1. Carninci, P.; Kasukawa, T.; Katayama, S.; Gough, J.; Frith, M. C., et al *Science* **2005**, *309*, 1559.
2. Katayama, S.; Tomaru, Y.; Kasukawa, T.; Waki, K.; Nakanishi, M., et al *Science* **2005**, *309*, 1564.
3. Krützfeldt, J.; Rajewsky, N.; Braich, R.; Rajeev, K. G.; Tuschl, T.; Manoharan, M.; Stoffel, M. *Nature* **2005**, *438*, 685.
4. Thuong, N. T.; Hélène, C. *Angew. Chem., Int. Ed. Engl.* **1993**, *32*, 666.
5. Ueno, Y.; Takeba, M.; Mikawa, M.; Matsuda, A. *J. Org. Chem.* **1999**, *64*, 1211.
6. Ueno, Y.; Mikawa, M.; Hoshika, S.; Matsuda, A. *Bioconjugate Chem.* **2001**, *12*, 635.
7. Ueno, Y.; Shibata, A.; Matsuda, A.; Kitade, Y. *Bioconjugate Chem.* **2003**, *14*, 684.
8. Rajeev, K. G.; Jadhav, V. R.; Ganesh, K. N. *Nucleic Acids Res.* **1997**, *25*, 4187.
9. Cuenoud; Casset, F.; Hüsken, D.; Natt, F.; Wolf, R. M.; Altmann, K. H.; Martin, P.; Moser, H. E. *Angew. Chem., Int. Ed.* **1998**, *37*, 1288.
10. Bijapur, J.; Keppler, M. D.; Bergqvist, S.; Brown, T.; Fox, K. R. *Nucleic Acids Res.* **1999**, *27*, 1802.
11. Ueno, Y.; Tomino, K.; Sugimoto, I.; Matsuda, A. *Tetrahedron* **2000**, *56*, 7903.
12. Atsumi, N.; Ueno, Y.; Kanzaki, M.; Shuto, S.; Matsuda, A. *Bioorg. Med. Chem.* **2001**, *10*, 2933.
13. Puri, N.; Majumdar, A.; Cuenoud, B.; Natt, F.; Matin, P.; Boyd, A.; Miller, P. S.; Seidman, M. M. *Biochemistry* **2001**, *41*, 7716.
14. Brazier, J. A.; Shibata, T.; Townsley, J.; Taylor, B. F.; Frary, E.; Williams, N. H.; Williams, D. M. *Nucleic Acids Res.* **2005**, *33*, 1362.
15. Radhakrishnan, I.; Patel, D. J. *Structure* **1993**, *1*, 135.
16. Giovannangeli, C.; Rougée, M.; Garestier, T.; Thuong, N. T.; Hélène, C. *Proc. Natl. Acad. Sci. U.S.A.* **1992**, *89*, 8631.
17. Malkov, V. A.; Voloshin, O. N.; Soyfer, V. N.; Frank-Kamenetskii, M. D. *Nucleic Acids Res.* **1993**, *21*, 585.